# Vibrational and thermal properties of Zn$X$ ($X$ = Se, Te): Density functional theory (LDA and GGA) versus experiment

R. K. Kremer,[1,*] M. Cardona,[1] R. Lauck,[1] G. Siegle,[1] and A. H. Romero[2]
[1]*Max-Planck-Institut für Festkörperforschung, Heisenbergstrasse 1, D-70569 Stuttgart, Germany*
[2]*CINVESTAV, Departamento de Materiales, Unidad Querétaro, Querétaro 76230, Mexico*
(Received 5 December 2011; published 19 January 2012)

We calculated the phonon dispersion relations of ZnX ($X$ = Se, Te) employing *ab initio* techniques. These relations have been used to evaluate the temperature dependence of the respective heat capacities of crystals with varied isotopic compositions. These results have been compared with measurements performed on crystals down to 2 K. The calculated and measured data are generally in excellent agreement with each other. Trends in the phonon dispersion relations and the corresponding densities of states for the zinc chalcogenide series of zinc-blende-type materials are discussed.

DOI: 10.1103/PhysRevB.85.035208 PACS number(s): 63.20.dk, 68.35.bg

## I. INTRODUCTION

In an ongoing effort to characterize the vibrational and thermal properties of multinary semiconductors and semimetals we have recently focused our attention on binary and ternary chalcogenides.[1–8] Most of our past experiments have been concerned with the heat capacities in the low-temperature regime where deviations from the Debye-$T^3$ power law can be easily studied. *Ab initio* density functional theory (DFT) calculations of the heat capacities ($C_v$) based on the electronic structure derived from local density functionals have been carried out and compared with the experimental results. By selective isotope substitution we effected incremental variations of the low-temperature heat capacity.[9] The small changes of these capacity are generally well described by DFT theory and were advantageously used to contrast the calculations with experimental data.

In the present contribution we extend our investigations to the thermal and vibrational properties of the binary semiconductors ZnSe and ZnTe. ZnSe and ZnTe crystallize at normal pressure and temperature in the cubic zinc-blende (zb) structure. ZnSe is a wide-band-gap II-VI semiconductor with a gap of 2.8 eV while the band gap of ZnTe is smaller and amounts to 2.2 eV. Because of its wide range the infrared optical transmittance of ZnSe has gained technological importance for application as optical components, such as windows or piezomodulators. ZnTe can be easily doped and has found applications in optoelectronics, e.g., for blue light-emitting diodes and solar cells as well as in nonlinear-optical devices.

The vibrational and thermal properties of ZnSe and ZnTe have been the subject of a number of studies. Initially the comparison of experimental data such as the phonon dispersion branches of ZnSe and ZnTe with inelastic neutron scattering (INS) (Refs. 10 and 11) or the heat capacity with theoretical approaches remained on the semiempirical level.[12–14] These early investigations have been extended recently to *ab initio* LDA and GGA calculations using up-to-date implementations of the DFT method. LDA results have been compared with the INS phonon energies and the heat capacity and found to be in good agreement.[15–17] Hamdi *et al.* have also calculated the structural parameters of ZnSe and compared them with experimental and other available theoretical data.[17] Recently, Tan *et al.* have used DFT-GGA calculations to study the pressure-induced phase transitions from the zb to the rocksalt structure.[18] They also performed calculations of the phonon dispersion relations and heat capacities of ZnSe and ZnTe with the DFT-GGA CASTEP code.[19] Unfortunately, the results of these calculations have not been compared in detail with the available experimental data.

Investigations of isotope substitution of the atomic masses of either Zn/(Se, Te) or simultaneously of both constituents simultaneously on the properties of Zn$X$ ($X$ = Se, Te) appear to be rather scarce. To the best of our knowledge, the only available study is a theoretical investigation of the temperature and mass dependence of the lattice constants, the temperature dependence of the linear thermal expansion coefficient, and the mode Grüneisen parameters upon isotopic substitution in ZnSe using perturbation theory in a density functional framework.[20] Also available is an experimental investigation of the Raman and excitonic spectra with different isotopic compositions.[21] In Ref. 21 an interesting dependence of the linewidth of the Raman spectra of ZnSe on isotope disorder was discovered.

We have recently demonstrated that changes of the heat capacity due to the isotope substitution, even though sometimes very small, can be revealed by careful experiments even on very small crystalline samples.[3] Especially, we have shown that the logarithmic derivatives with respect to the atomic masses $m_i$, $d\ln(C_p/T^3)/d\ln m_i$, are a very sensitive and useful tool to highlight small alterations of the heat capacities since the logarithmic derivative eliminates, to a large extent, systematic experimental errors. In binary and multinary compounds the logarithmic derivatives particularly allowed us to reveal the influence of variations of the atomic masses on the phonon spectrum and to compare with the calculated phonon density of states (PDOS). We have also proposed and tested a sum rule which relates the sum of the logarithmic derivatives of $C_p/T^3$ with respect to the atomic masses with the logarithmic derivative with respect to temperature.[23]

The low-temperature heat capacity of ZnSe has been the subject of two preceding experimental studies carried out in the 1970s by Irwin and LaCombe[24] and by Birch.[25] However, the two previous heat capacity data sets just overlap in the temperature range of the $C_p/T^3$ maximum which for ZnSe occurs at about 20 K: In order to enable a meaningful comparison, e.g., with the logarithmic derivatives, and to test

 

the sum rule a repetition of the measurements on a ZnSe sample with natural isotope composition was found necessary. We therefore carried out measurements of the heat capacity on a series of samples with various isotope combinations with special emphasis on the low-temperature regime. For ZnTe, heat capacity data are available only down to ∼15 K,[24,26,27] but the data from the different authors deviate significantly from each other, especially in the temperature regime where the maximum in $C_p/T^3$ is expected. We therefore repeated and extended the heat capacity measurement on ZnTe down to ∼2 K. Our measurements reveal clearly the maximum in $C_p/T^3$ at ∼14 K. Additionally, our low-temperature heat capacity data enable us to extract very reliably the Debye temperatures for $T \rightarrow 0$ K, $\Theta_{\mathrm{Debye}}(0)$, for ZnSe and ZnTe.

The comparison of our experimental data and literature data of the phonon dispersion obtained by INS experiments with the calculations shows significantly better agreement with the LDA while the GGA data deviate noticeably from the experiments. The analysis of the total and the partial phonon densities of states and the comparison with that of ZnS (Ref. 4) highlights the close similarities of the PDOS of Zn$X$ ($X$ = S, Se, Te). It also reveals the compression of the frequency scales with increasing mass of the chalcogen atom. The PDOSs projected on the Zn and the $X$ atoms exhibits an interesting trend upon going from S to Te. While in ZnS the acoustical and optical phonons can be clearly attributed to vibrations of the Zn and S atoms, respectively, the situation is reversed for ZnTe. Here the optical branches emerge essentially from vibrations of the lighter Zn atoms. For ZnSe, with almost equal masses of the Zn and the Se atoms, the acoustical and optical phonon branches arise from combined vibrations of Zn and Se, respectively.

## II. THEORETICAL DETAILS

For the calculations reported here we have made use of density functional theory[28,29] as implemented in the ABINIT package.[30] Two different exchange-correlation functionals (LDA, GGA) were tested but most of our results are based on the LDA approach, basically because it gives a much better agreement with experimental data.

In the ABINIT package we have utilized a linear response approach[31–33] together with an iterative minimization norm-conserving pseudopotential plane-wave method.[34] These pseudopotentials are single projector, ordinary norm conserving, based on the Troullier-Martins method.[35–37] Twelve and six "valence" electrons were used for Zn and Se, respectively. A 40 Ry cutoff was set for the plane-wave expansion and an 8×8×8 **k**-point grid regularly shifted along four different directions, with a total of 60 **k** points for the ground-state calculation and 2048 **k** points for the vibrational response part. The calculations converged well: Increasing the plane-wave cutoff to 50 Ry and the **k**-points mesh to 10×10×10 yielded, on average, a change of less then two percent in the phonon frequencies. For the phonon frequencies we have used a **q** mesh of 12×12×12, to guarantee a good coverage of the dispersion relations. The dynamical matrices were obtained from perturbation theory[32,33] and a Fourier interpolation was employed in order to increase the mesh sampling and to improve the description of quantities such as vibrational density of states and heat capacities.

## III. EXPERIMENTAL

zb-ZnSe and zb-ZnTe crystals with different isotopic compositions—$^{\mathrm{nat}}$Zn $^{\mathrm{nat}}$Se/Te, i.e., Zn and Se/Te with natural isotope composition, $^{64}$Zn $^{76}$Se, $^{64}$Zn $^{80}$Se, $^{68}$Zn $^{76}$Se, $^{68}$Zn $^{80}$Se, $^{68}$Zn $^{\mathrm{nat}}$Te, and $^{\mathrm{nat}}$Zn $^{130}$Te—were grown by vapor phase transport as described in detail previously.[38] Larger zb-ZnTe crystals with the natural isotope composition were obtained by a modified Piper-Polich method in a semiopen quartz-glass ampoule.[39,40] The heat capacities of crystalline pieces of these samples, typically of ∼20–100 mg weight, were measured between 2 and 280 K with a physical property measurement system (Quantum Design, San Diego, CA) as described in detail in Ref. 41.

## IV. LATTICE DYNAMICS

In Figs. 1(a) and 1(b) we display the calculated phonon dispersion relations of ZnSe along selected directions of the Brillouin zone (BZ). For comparison we have plotted our LDA and GGA results and the INS data reported by Hennion *et al.*[10] The LDA calculations are overall in good agreement with the experimental findings, as has also been observed by Dal Corso *et al.*[15] The results of the GGA calculation deviate markedly, especially for the optical branches.

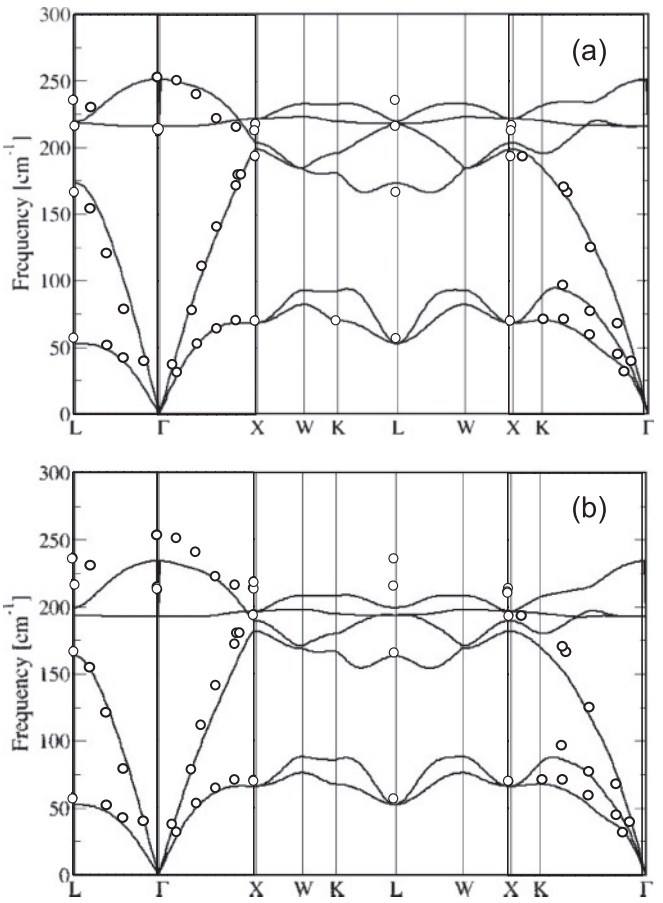


FIG. 1. Phonon dispersion relations of ZnSe as obtained by DFT-LDA (a) and DFT-GGA (b) calculations. The circles represent the inelastic neutron scattering data measured by Hennion *et al.* (Ref. 10).

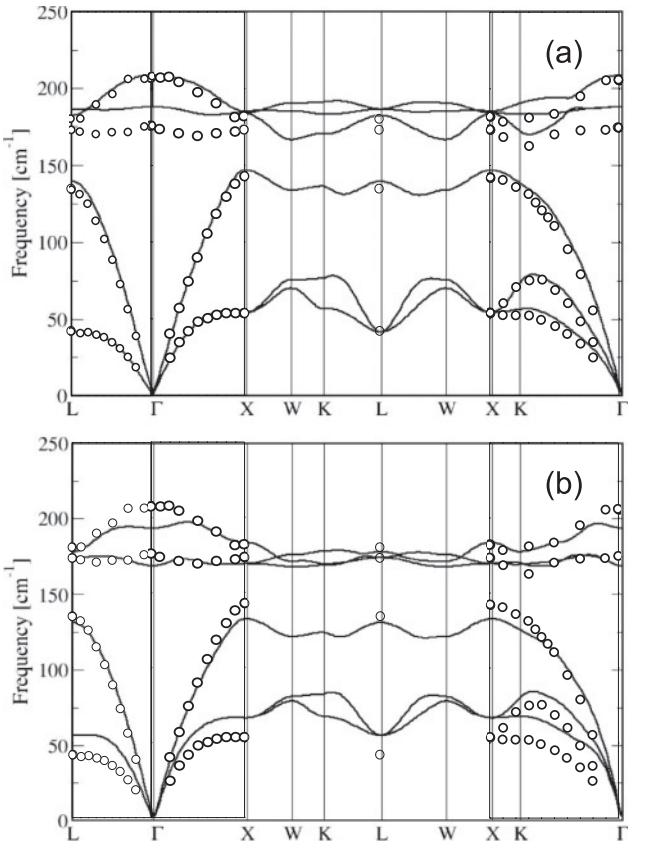


FIG. 2. Phonon dispersion relations of ZnTe as obtained by DFT-LDA (a) and DFT-GGA (b) calculations. The circles represent the inelastic neutron scattering data measured by Vagelatos *et al.* (Ref. 11).

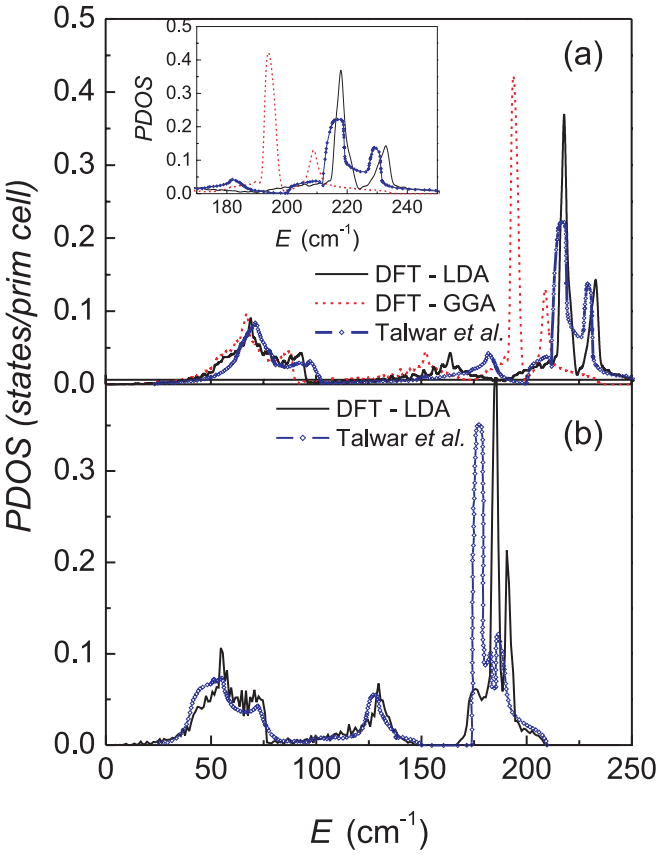


FIG. 3. (Color online) One-phonon density of states (PDOS) of (a) ZnSe and (b) ZnTe as obtained by DFT-LDA and DFT-GGA calculations. The diamonds represent data by Talwar *et al.* (Ref. 13). The inset displays the high-energy section in an enlarged scale.

Figures 2(a) and 2(b) show the comparison of the LDA and GGA calculations for ZnTe with the INS data collected by Vagelatos *et al.*[11] As already observed by Dal Corso *et al.* the agreement of the experiment with the DFT-LDA calculations is excellent, especially for the acoustical branches. The longitudinal optical branches are equally well reproduced by the calculations, while the transverse optical branches fall short by about 5%. The DFT-GGA results agree well with the optical branches while the energies of transverse acoustical branches lie systematically below the experimental data.

The total PDOS and the PDOS projected on the two constituting elements as obtained by the LDA calculations are displayed in Fig. 3. For comparison we also show the PDOS of ZnSe and ZnTe derived by Talwar *et al.* from a rigid-ion model.[13] In Fig. 4 we also added the PDOS of ZnS as published by us recently.[4] Very similar to the PDOS of ZnS the PDOSs of ZnSe and ZnTe exhibit two dominating features, one between 50 and 100 cm$^{-1}$, arising essentially from acoustic phonon branches, and a sharp double peak at higher energies corresponding to the the optical phonons. The energies of the latter peaks decrease markedly as one substitutes S by Se and Te. These two main peak groups are separated by a gap in which a small midgap peak is located. While the low-energy peak in the PDOS of ZnSe is largely independent of the computational approach the midgap feature and the sharp optical phonon double peak obtained from the GGA calculations are downshifted, the latter by about 10% as compared to the LDA result. Except for the midgap peak the LDA PDOS is generally in good agreement with results of the rigid-ion model used by Talwar *et al.*[13]

It is of interest to compare the projected PDOS of the three systems Zn$X$ ($X$ = S, Se, Te) (see Fig. 4). For the ZnS the acoustical and the high-energy optical phonon branches arise essentially from vibrations of Zn and S, respectively. Due to the reversal of the masses of the two constituents in ZnTe (Zn: ∼65 a.m.u.; Te: ∼128 a.m.u) the situation is reversed for ZnTe. There the acoustical phonons arise from Te vibrations and the optical ones from vibrations of the lighter Zn atoms. Due to the similar atomic masses of Zn and Se acoustical and optical phonon branches for ZnSe comprise mixed Zn and Se vibrations.

## V. HEAT CAPACITY

By using the calculated PDOS($\omega$) we obtained the free energy $F(T)$ and the heat capacity (at constant volume) $C_v(T)$ according to[22]

$$F(T) = -\int_0^\infty \left\{\frac{\hbar\omega}{2} + k_B T \ln[2n_B(\omega)]\right\} \mathrm{PDOS}(\omega) d\omega, \quad (1)$$

$$C_v(T) = -T\left(\frac{\partial^2 F}{\partial T^2}\right)_V, \quad (2)$$

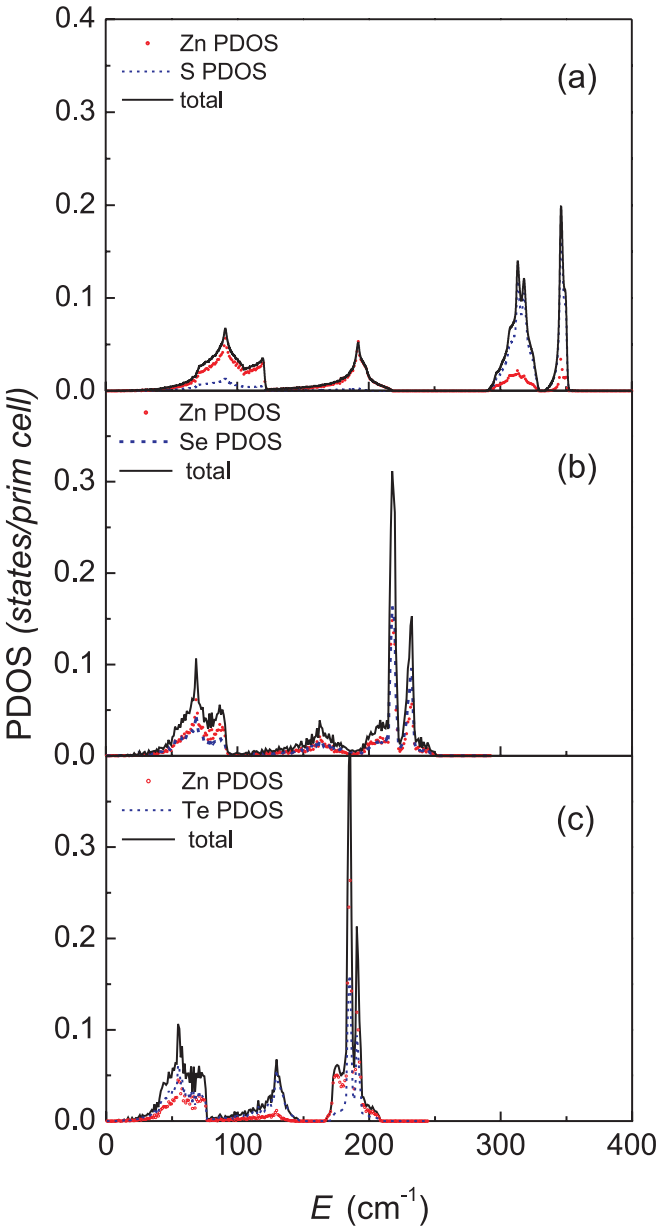


FIG. 4. (Color online) Comparison of the one-phonon density of states (PDOS) of (a) ZnS (Ref. 4), (b) ZnSe, and (c) ZnTe as obtained by DFT-LDA calculations. The decomposition into contributions from Zn and from the chalcogen is also given (Ref. 13).

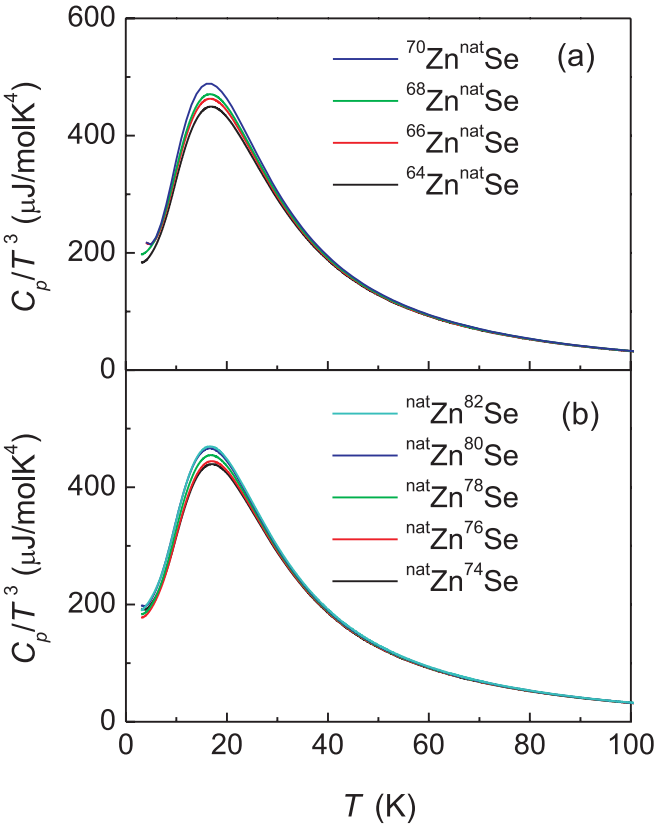


FIG. 5. (Color online) Calculated low-temperature heat capacity of ZnSe (ABINIT DFT-LDA) assuming different masses for the Zn and the Se isotopes, as given in the insets (increasing isotope mass from bottom to top).

where $k_B$ is the Boltzmann constant and $n_B$ the Bose-Einstein factor. The cutoff in PDOS($\omega$) at the highest phonon frequency defines the upper limit of integration.

Figures 5 and 6 display the calculated heat capacities, $C_p(T) \approx C_v(T)$,[22] of ZnSe and ZnTe for different isotope mass compositions in the $C_p/T^3(T)$ representation which is chosen to emphasize the broad peak at low temperature. For ZnSe the maximum is found at 17.2 K and for ZnTe it moves down to 13.5 K. The broad peak in the $C_p/T^3(T)$ representation of the heat capacity has been demonstrated to arise from regions of low dispersion of zone-boundary acoustical phonons which also give rise to the low-energy peaks in the PDOS.[23] They appear at 68.6 $cm^{-1}$ and 55.1 $cm^{-1}$ for ZnSe and ZnTe, respectively. We again find a ratio ~6 for the energies of the acoustical phonon peaks and the temperatures of the peaks in the $C_p/T^3(T)$ representation, close to what has been typically observed for several semiconductors before.[3]

The peak value of $C_p/T^3$(~13.5 K) for ZnTe is by almost a factor of two larger than that of ZnSe at 17.2 K, reflecting the lattice softening when Se is replaced by Te. Isotope mass increases lead to small growth of the heat capacity, which becomes clearly visible as slight changes of the maximum value of the $C_p/T^3(T)$ peak. Below we will discuss the logarithmic derivatives of $C_p/T^3(T)$ which reveal that the variation of the isotope masses changes the heat capacity in different temperature regimes. Figure 7 displays the logarithmic derivatives, $d\ln(C_p/T^3)/d\ln m_i$, with respect to the isotope mass, $m_i$, of the two constituting elements, Zn and either Se or Te, respectively. For completeness we have also included the similar graphs for ZnS.[4] For the latter there is a clear differentiation between the derivative vs the masses of Zn and S. Similar sharp peaks at low temperature, with that of S significantly smaller in magnitude than that of the Zn derivative, have been attributed to a considerable S component in the TA vibrations which have mainly Zn character. The characteristic S contribution due to high-energy S vibrations shows up as a broad peak centered near 100 K.[4] Similar derivatives are obtained for ZnSe and ZnTe. However, depending on the relative masses of the constituents Zn and Se/Te the magnitude and the maximum temperatures of the peaks shift. For ZnSe the low-temperature peaks in

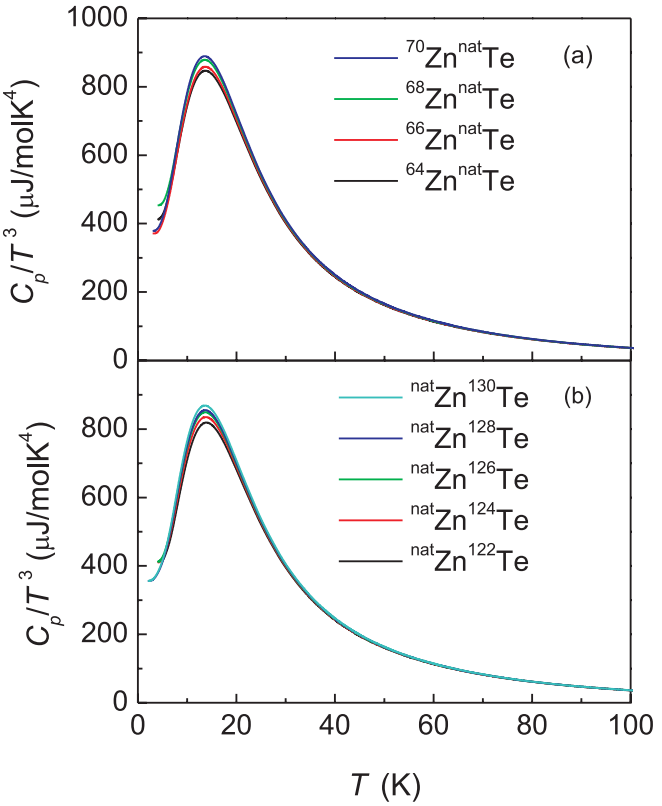


FIG. 6. (Color online) Calculated low-temperature heat capacity of ZnTe (ABINIT DFT-LDA) assuming different masses for the Zn and the Te isotopes, as given in the insets (increasing isotope mass from bottom to top).

the derivative are of equal magnitude and a pronounced high-temperature peak is missing. This finding reflects the mixing of Zn- and Se-related vibrations due to the rather similar atomic masses of Zn and Se. For ZnTe the situation is reversed. Here the pronounced peak at low temperature is associated with Te vibrations, while the vibrations of the lighter Zn atoms give rise to a shallow broad peak centered at ∼70 K. Again, as in ZnS, there is some hybridization of Zn with Te vibrations and a noticeable Zn component in the TA vibrations which now have mainly Te character.

In previous work we have demonstrated that for low temperatures, $T \to 0$, the logarithmic derivatives versus mass are related to the ratios of the atomic mass to the molar mass according to[4,5,41]

$$\frac{d\ln(C_p/T^3)}{d\ln m_{\mathrm{Zn}}} = \frac{3}{2}\frac{m_{\mathrm{Zn}}}{m_{\mathrm{Zn}}+m_X} = 0.68\ (\mathrm{Se});\ = 0.51\ (\mathrm{Te}), \tag{3}$$

$$\frac{d\ln(C_p/T^3)}{d\ln m_X} = \frac{3}{2}\frac{m_X}{m_{\mathrm{Zn}}+m_X} = 0.82\ (\mathrm{Se});\ = 0.99\ (\mathrm{Te}). \tag{4}$$

The dashed lines at low temperatures in Fig. 7 represent a free-hand extrapolation for $T \to 0$ so as to agree with these values.

Our low-temperature heat capacities of ZnSe and ZnTe collected on samples with the natural isotope composition are summarized and compared with the results of the DFT-LDA and GGA calculations in Fig. 8. The $C_p/T^3$ representation reveals low-temperature peaks at 17.0 K and at 13.5 K, for ZnSe and ZnTe, respectively. For ZnSe the data by Irwin *et al.*[24] and Birch[25] are in good agreement with our more complete data. Especially, for ZnTe we were able to clarify differences in the low-temperature heat capacity results obtained before by Gavrichev *et al.*[27] and Irwin *et al.*[24] and extend the temperature range down to 2 K. This was found necessary in order to clearly establish the position and magnitude of the $C_p/T^3$ maximum and to enable the calculation of the logarithmic derivatives, discussed below.

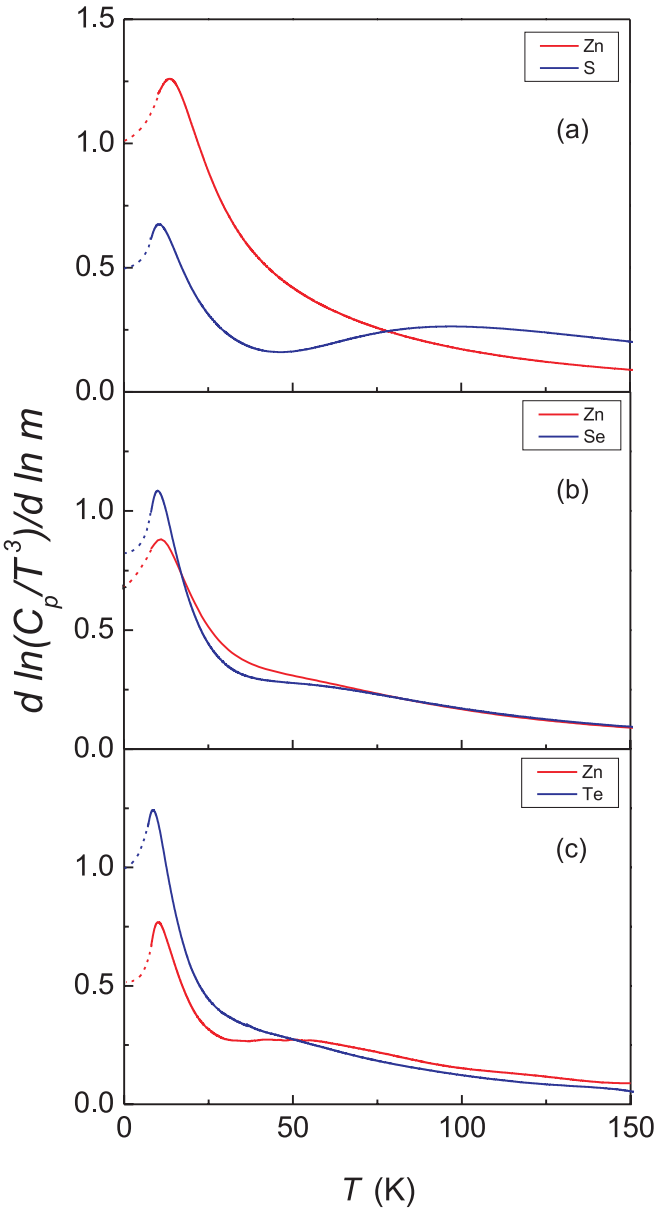


FIG. 7. (Color online) Logarithmic derivatives vs the masses of the constituents, Zn (solid red) and $X$ [$X$ = S, Se, Te; solid blue lines in (a), (b), and (c), respectively] calculated from the LDA heat capacity results displayed in Figs. 5 and 6. The ZnS data (a) were taken from Ref. 4. The dashed parts of the calculated curves have been extrapolated by free hand so as to agree with the value of Eqs. (3) and (4) at $T = 0$.

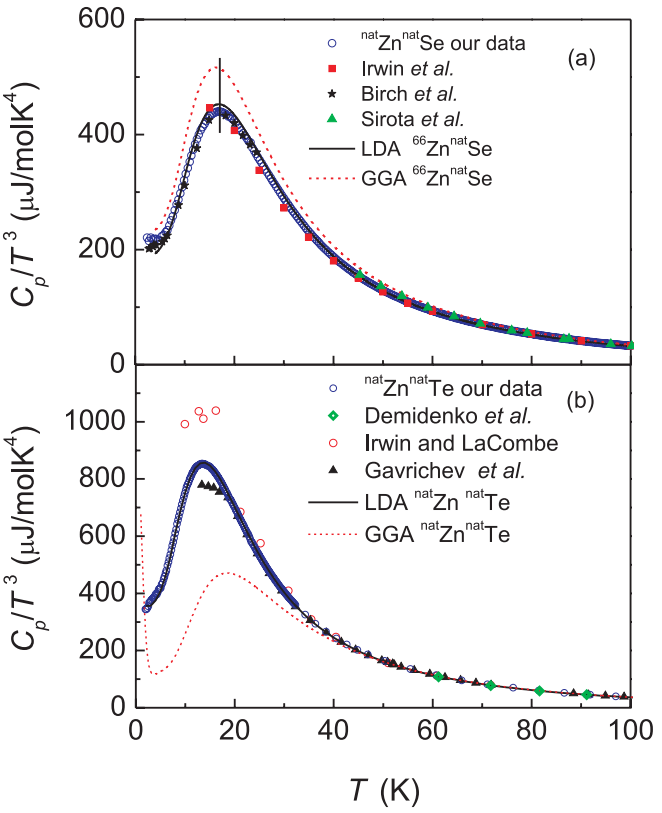


FIG. 8. (Color online) Our experimental results and literature data of the low-temperature heat capacities of (a) ZnSe and (b) ZnTe compared with the ABINIT DFT-LDA and GGA results, (black) solid and (red) dashed lines, respectively. For the references of the literature data see text.

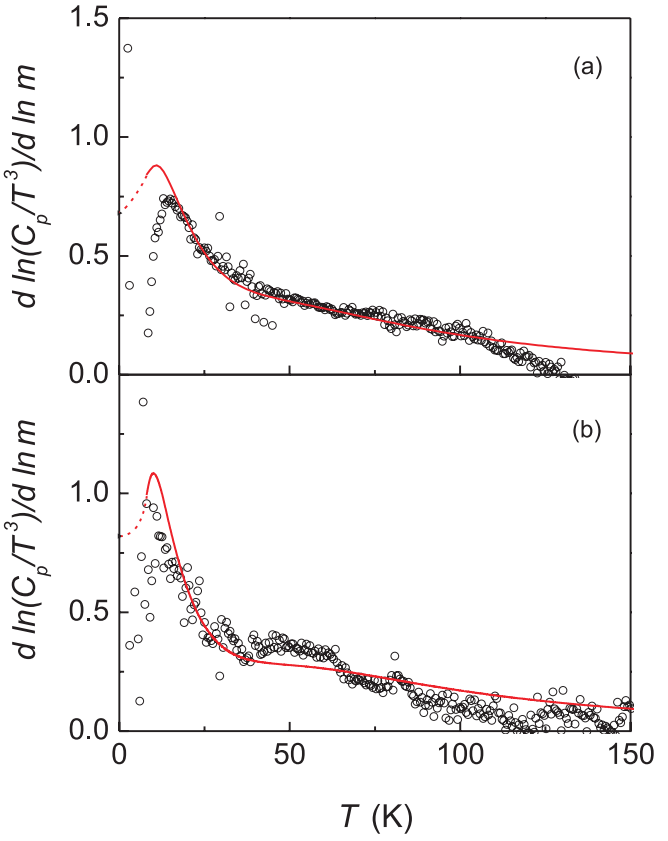


FIG. 9. (Color online) Logarithmic derivative of $C_p/T^3$ of ZnSe vs the isotope masses of (a) Zn and (b) Se. Circles show experimental results, (red) solid line LDA calculations. The (red) dashed lines are free-hand extrapolations (see Fig. 7).

The Debye temperatures, $\theta_{\rm Debye}(0)$, for $T \to 0$ K were obtained by fitting a power law $C_p/T = \beta T^2 + \delta T^4$ to the experimental data in the temperature range 2 K $\leqslant T \leqslant$ 10 K. The fitted coefficient $\beta$ is related to $\theta_{\rm Debye}(0)$ according to $\beta = 12/5\pi^4 nR[1/\theta_{\rm Debye}(0)]^3$, where $R$ is the molar gas constant and $n = 2$ is the number of atoms per formula unit.

For ZnSe we found

$$\theta_{\rm Debye}(0) = 289(2)\ {\rm K}\ \ {\rm for}\ \ {\rm ZnSe},$$

which is by about 6% larger than the value reported by Birch[25] and somewhat closer to the result (278.5 K) derived from the elastic constants by Lee.[42]

For ZnTe we obtained

$$\theta_{\rm Debye}(0) = 230(2)\ {\rm K},$$

which is close to the value from elastic constants measurements (225.3 K)[42] but significantly larger than the values estimated from x-ray measurements and quoted in review articles (182–210 K).[43,44]

We finally note that the ratio of the Debye temperatures, 1.26, is very close to the square-root of the inverse atomic mass ratio of the chalcogenide atoms,

$$\theta_{\rm Debye}(0)_{\rm ZnSe}/\theta_{\rm Debye}(0)_{\rm ZnTe} \approx \sqrt{m_{\rm Te}/m_{\rm Se}} = 1.27.$$

As already observed for the phonon dispersion, the agreement of the heat capacities of ZnSe and ZnTe with the LDA calculations is better than with the GGA results. Especially in the temperature regime of the $C_p/T^3$ maximum, GGA overestimates (underestimates) the experimental data by about 20% (50%) for ZnSe (ZnTe).

The logarithmic derivatives vs the mass of the isotopes of Zn and Se are summarized in Fig. 9. Those for Zn and Te are displayed in Fig. 10. The agreement with the LDA calculations in magnitude and position of the low-temperature peaks is rather satisfactory. For ZnTe, the logarithmic derivative with respect to the isotope mass of the Zn atoms clearly exhibits the broad maximum centered at ~50 K due to phonons involving low-energy Zn vibrations.

In previous work on monatomic crystals we derived a connection between the logarithmic derivative of $C_p/T^3$ versus $T$ and the corresponding derivative vs the isotopic mass.[9] For binary and ternary materials, a similar connection was shown to hold provided one adds the two or three logarithmic derivatives with respect to each of the isotope masses.[5,23]

Accordingly, for the relation of the temperature and isotope mass derivatives in a two-component system we obtain the expression[2]

$$\frac{1}{2}\left(3 + \frac{d\ln[C_p(T)/T^3]}{d\ln T}\right) = \sum_{i=1}^{2} \frac{d\ln[C_p(T)/T^3]}{d\ln m_i}, \quad (5)$$

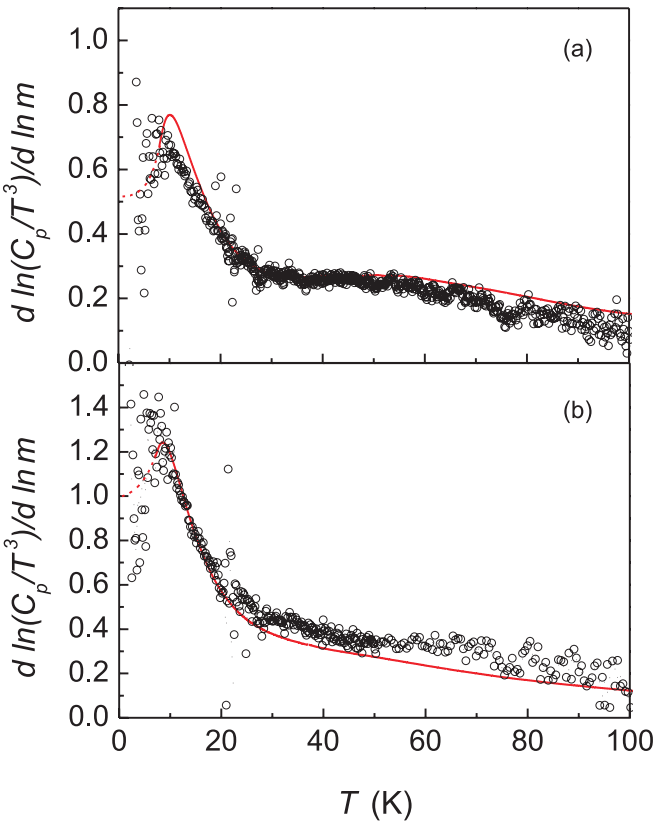


FIG. 10. (Color online) Logarithmic derivative of $C_p/T^3$ of ZnTe vs the isotope masses of (a) Zn and (b) Te. Circles show experimental results, (red) solid line LDA calculations. The (red) dashed lines are free-hand extrapolations (see Fig. 7).

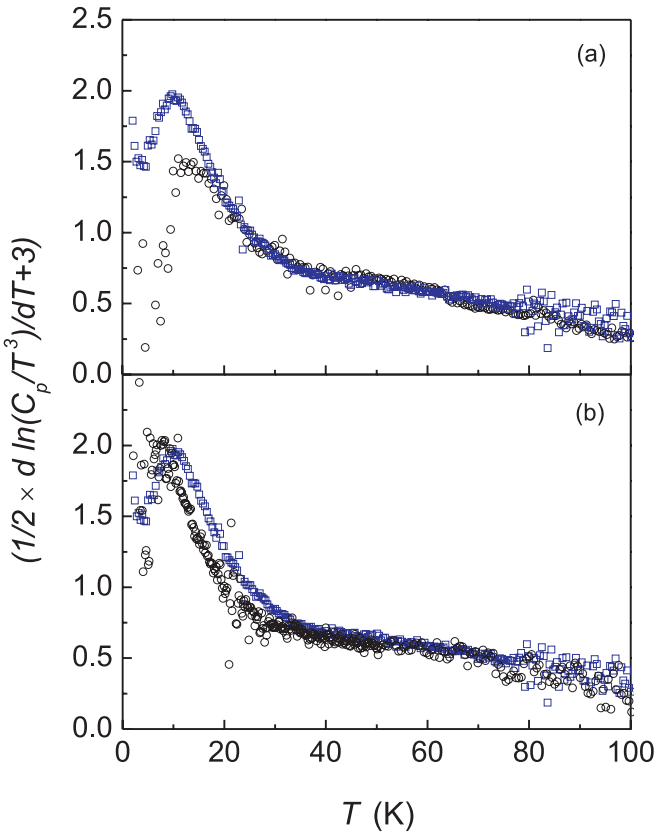


FIG. 11. (Color online) Comparison and sum rule [Eq. (5)] for (a) ZnSe and (b) ZnTe. The circles and the squares represent the right-hand side and left-hand side of Eq. (5), respectively.

where $m_i$ ($i = 1, 2$) are the masses of the two constituting elements, i.e., Zn and $X$ = Se and Te, respectively. As demonstrated in Fig. 11, the relation given in Eq. (5) is nicely fulfilled for ZnSe and ZnTe, thus lending further support for the proposed sum rule.

## VI. CONCLUSIONS

Up-to-date *ab initio* electronic structure calculations have now matured and become a powerful tool to study the thermodynamic properties of crystals. Here we demonstrate this for the binary zinc chalcogenides, ZnSe and ZnTe. Both materials are technologically important semiconductors used for optical applications. We have used DFT-LDA and GGA codes to calculate the phonon dispersions and the heat capacities down to the lowest temperatures. In the experimental part we extend the available experimental basis and comprehensively determine the heat capacities of ZnSe and ZnTe over the temperature range from 2 K to room temperature and have compared the results with the calculations. Generally, better agreement of the experimental data is found with the DFT-LDA results. Additionally, we measured the heat capacities of isotope-substituted samples in order to vary the atomic masses of Zn and Se and Te and to probe the effect of selective isotope substitution on the phonon spectra and the thermodynamic properties. These data are compared with the results of the calculations and found to be in very good agreement. A comparison of ZnS, ZnSe, and ZnTe instructively reveals the variation of the phonon spectrum with the variation of the atomic mass of chalcogenide atoms.

## ACKNOWLEDGMENTS

A.H.R. has been supported by CONACYT Mexico under projects J-152153-F, Binational Collaboration FNRS-Belgium-CONACYT, and PPPROALMEX-DAAD-CONACYT. We are indebted to G. Bester for a critical reading of the manuscript.

*Corresponding author: r.kremer@fkf.mpg.de

[1]M. Cardona, R. K. Kremer, R. Lauck, G. Siegle, A. Muñoz, and A. H. Romero, Phys. Rev. B **80**, 195204 (2009).

[2]A. H. Romero, M. Cardona, R. K. Kremer, R. Lauck, G. Siegle, J. Serrano, and X. C. Gonze, Phys. Rev. B **78**, 224302 (2008).

[3]M. Cardona, R. K. Kremer, G. Siegle, A. Muñoz, A. H. Romero, and M. Schmidt, Phys. Rev. B **82**, 085210 (2010).
[4]M. Cardona, R. K. Kremer, R. Lauck, G. Siegle, A. Muñoz, A. H. Romero, and A. Schindler, Phys. Rev. B **81**, 075207 (2010).
[5]A. H. Romero, M. Cardona, R. K. Kremer, R. Lauck, G. Siegle, C. Hoch, A. Muñoz, and A. Schindler, Phys. Rev. B **83**, 195208 (2011).
[6]R. K. Kremer, M. Cardona, E. Schmitt, J. Blumm, S. K. Estreicher, M. Sanati, M. Bockowski, I. Grzegory, T. Suski, and A. Jezowski, Phys. Rev. B **72**, 075209 (2005).
[7]L. E. Diaz-Sanchez, A. H. Romero, M. Cardona, R. K. Kremer, and X. Gonze, Phys. Rev. Lett. **99**, 165504 (2007).
[8]J. Serrano, R. K. Kremer, M. Cardona, G. Siegle, L. E. Diaz-Sanchez, and A. H. Romero, Phys. Rev. B **77**, 054303 (2008).
[9]A. Gibin, G. G. Devyatykh, A. V. Gusev, R. K. Kremer, M. Cardona, and H.-J. Pohl, Solid State Commun. **133**, 569 (2005).
[10]B. Hennion, F. Moussa, G. Pepy, and K. Kunc, Phys. Lett. A **36**, 376 (1971).
[11]N. Vagelatos, D. Wehe, and J. S. King, J. Chem. Phys. **60**, 3613 (1974).
[12]P. Plumelle and M. Vandevyer, Phys. Status Solidi B **73**, 271 (1976).
[13]D. N. Talwar, M. Vandevyver, K. Kunc, and M. Zigone, Phys. Rev. B **24**, 741 (1981).
[14]A. K. Kushwaha, Physica B **405**, 1638 (2010).
[15]A. Dal Corso, S. Baroni, R. Resta, and S. de Gironcoli, Phys. Rev. B **47**, 3588 (1993).
[16]K. Petzke, C. Schrepel, and U. Scherz, Z. Phys. Chem. **201**, 317 (1997).
[17]I. Hamdi, M. Aouissi, A. Qteish, and N. Meskini, Phys. Rev. B **73**, 174114 (2006).
[18]Tan Jia-Jin, Ji Guang-Fu, Chen Xiang-Rong, and Guo Quing-Quan, Commun. Theor. Phys. (Beijing) **53**, 1160 (2010).
[19]For reference see the CASTEP website at [http://www.castep.org/].
[20]A. Debernardi and M. Cardona, Phys. Rev. B **54**, 11305 (1996).
[21]A. Göbel, T. Ruf, J. M. Zhang, R. Lauck, and M. Cardona, Phys. Rev. B **59**, 2749 (1999).
[22]As discussed in Ref. 6, the difference between the experimentally accessible heat capacity at constant pressure, $C_p$, and $C_v$ is significant only at high temperatures and thus negligible in the low-temperature range considered here.
[23]M. Cardona, R. K. Kremer, R. Lauck, G. Siegle, J. Serrano, and A. H. Romero, Phys. Rev. B **76**, 075211 (2007).
[24]J. C. Irwin and J. LaCombe, J. Appl. Phys. **45**, 567 (1974).
[25]J. A. Birch, J. Phys. C **8**, 2043 (1975).
[26]A. F. Demidenko and A. K. Maltsev, Izv. Akad. Nauk SSSR Neorg. Mater. **5**, 158 (1969) [Inorg. Materials **5**, 130 (1969)].
[27]K. S. Gavrichev, G. A. Sharpataya, V. N. Guskov, J. H. Greenberg, T. Feltgen, M. Fiederle, and K. W. Benz, Phys. Status Solidi B **229**, 133 (2002).
[28]P. Hohenberg and W. Kohn, Phys. Rev. **136**, B864 (1964).
[29]W. Kohn and L. J. Sham, Phys. Rev. **140**, A1133 (1965).
[30]X. Gonze, B. Amadon, P.-M. Anglade, J.-M. Beuken, F. Bottin, P. Boulanger, F. Bruneval, D. Caliste, R. Caracas, M. Cote, T. Deutsch, L. Genovese, Ph. Ghosez, M. Giantomassi, S. Goedecker, D. R. Hamann, P. Hermet, F. Jollet, G. Jomard, S. Leroux, M. Mancini, S. Mazevet, M. J. T. Oliveira, G. Onida, Y. Pouillon, T. Rangel, G.-M. Rignanese, D. Sangalli, R. Shaltaf, M. Torrent, M. J. Verstraete, G. Zerah, and J. W. Zwanziger, Comput. Phys. Commun. **180**, 2582 (2009); ABINIT is a common project of the Universite Catholique de Louvain, Corning Incorporated, and other contributors [http://www.abinit.org/].
[31]S. Baroni, P. Giannozzi, and A. Testa, Phys. Rev. Lett. **58**, 1861 (1987).
[32]X. Gonze, Phys. Rev. B **55**, 10337 (1997).
[33]X. Gonze and C. Lee, Phys. Rev. B **55**, 10355 (1997).
[34]X. Gonze, J. M. Beuken, R. Caracas, F. Detraux, M. Fuchs, G. M. Rignanese, L. Sindic, M. Verstraete, G. Zerah, and F. Jollet, Comput. Mater. Sci. **25**, 478 (2002).
[35]D. R. Hamann, M. Schluter, and C. Chiang, Phys. Rev. Lett. **43**, 1494 (1979).
[36]N. Troullier and J. L. Martins, Phys. Rev. B **43**, 1993 (1991).
[37]M. C. Payne, M. P. Teter, D. C. Allan, T. A. Arias, and J. D. Joannopoulos, Rev. Mod. Phys. **64**, 1045 (1992).
[38]R. Lauck and E. Schönherr, J. Cryst. Growth **197**, 513 (1999).
[39]R. Lauck and G. Müller-Vogt, J. Cryst. Growth **74**, 513 (1986).
[40]R. Lauck, G. Müller-Vogt, and W. Wendl, J. Cryst. Growth **74**, 520 (1986).
[41]J. Serrano, R. K. Kremer, M. Cardona, G. Siegle, A. H. Romero, and R. Lauck, Phys. Rev. B **73**, 094303 (2006).
[42]B. H. Lee, J. Appl. Phys. **41**, 2984 (1970).
[43]See R. J. Blattner, L. K. Walford, and T. O. Baldwin, J. Appl. Phys. **43**, 935 (1972) for detailed references.
[44]*Semiconductors: II-VI and I-VII Compounds; Semimagnetic Compounds*, edited by U. Rössler, Landolt-Börnstein, New Series, Group III, Vol. 41, Part B (Springer, New York, 1999).